Available online at www.sciencedirect.com
SCIENCE DIRECT®
ELSEVIER
International Journal of Solids and Structures 42 (2005) 4204–4219
INTERNATIONAL JOURNAL OF SOLIDS and STRUCTURES
www.elsevier.com/locate/ijsolstr

Behavior of a structurally dissipating rock-shed: experimental analysis and study of punching effects

F. Delhomme [a,b,*], M. Mommessin [a], J.P. Mougin [a], P. Perrotin [a,*]

[a] *Design Optimization and Environmental Engineering Laboratory (LOCIE-ESIGEC), RNVO, University of Savoie, 73376 Le Bourget du Lac, France*
[b] *Tonello I.C. Office, 73102 Aix Les Bains, France*

Received 6 May 2004; received in revised form 8 December 2004
Available online 26 January 2005

Abstract

This article is about protective structures against rock fall. We present a new concept of rock-shed protection: it consists of a reinforced concrete slab (not protected by any ground embankment) supported by specific supports designed to dissipate the energy of blocks hitting on the edge of the slab. The impact energy is dissipated directly by the actuation of the slab and by the damage concrete and reinforcements or by the buckling of the fuse supports. Unlike traditional rock-shed (covered in soil), this new kind of structure must be designed under dynamic load. Experimental trial runs have been conducted on a one-third scale model of a real structure. It appears that three damaging modes have to be considered: the "concrete compaction", punching and bending of the slab. In this paper, we focus on the punching effects. In order to propose a simplified design method, we have determined the experimental value of contact time and percussion load. Then, this load is compared with the ultimate punching load of the slab computed by an analytical model (Menétrey) and a standard code (Eurocode 2). It results that whenever the percussion load is higher than the ultimate punching load, the slab has been strongly punched.

Keywords: Rock-shed; Reinforced concrete; Impact; Punching; Percussion; Slab

1. Introduction

Among the usual hazards in mountainous areas, accidental rock fall often causes a lot of damage: unusable roads or railway lines, destroyed infrastructures, etc., which can considerably affect the economic

* Corresponding authors. Address: LOCIE-ESIGEC, GCH, University of Savoie—LOCIE, 73376 LE BOURGET DU LAC, France. Tel.: +33 4 79 75 88 21; fax: +33 4 79 75 81 44 (F. Delhomme).
E-mail addresses: fabien.delhomme@univ-savoie.fr (F. Delhomme), pascal.perrotin@univ-savoie.fr (P. Perrotin).

0020-7683/$ - see front matter © 2004 Elsevier Ltd. All rights reserved.
doi:10.1016/j.ijsolstr.2004.12.008

activity in these areas. Against the hazard of rock fall, there are two kinds of protection: active ones (like nets) and passive ones. Rock-shed structures are regarded as passive protection.

The technique usually used to build rock-shed structures consists in setting up, above the road, a slab covered with a ground embankment (Fig. 1) in the zone exposed to falling blocks. This embankment acts as a shock absorber, which permits the calculation of the slab under static loading (Masuya and Labiouse, 1999). Unfortunately, this technology has many disadvantages; the most important one is the heavy deadweight of the structure which requires massive foundations. Moreover, the evacuation of the fallen blocks, the replacement of the embankment and repairs are difficult, even impossible to carry out.

Japanese research (Ikeda et al., 1999) has also been led on an absorbing system called three layered absorbing system (TLAS). It is composed of a 50 cm thick sand layer (top), a 20–30 cm thick reinforced concrete slab (core) and a 50–100 cm thick Expanded Poly-styrol block (bottom). Impact tests were performed with a steel weight of 49 kN dropped from a height of 40 m. This structure has the advantage of reducing the impact effort on the slab but remains complicated to realize and rock-sheds are often built in zones where access is difficult (mountainous areas). Moreover, repair is difficult to realize and the problem of the shocks on the level of the supports is not discussed.

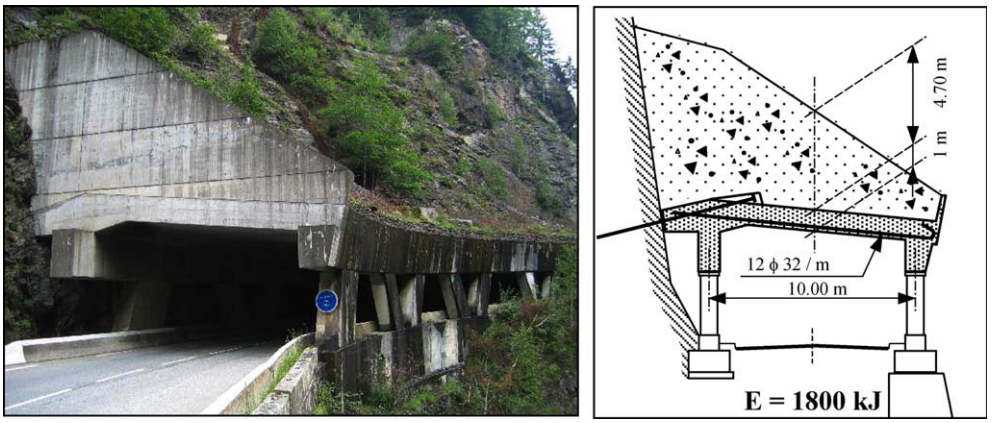

Fig. 1. Conventional solution.

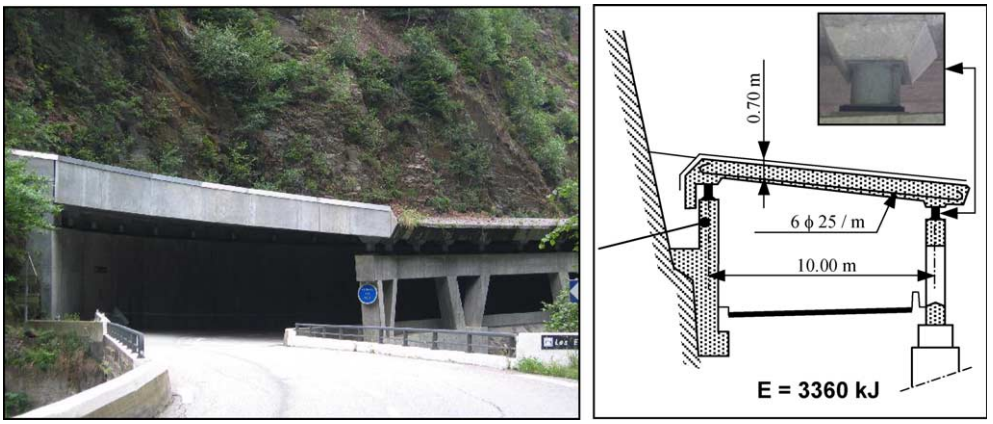

Fig. 2. New concept (structurally dissipating rock-shed).

Table 1
Comparison between an SDR and a conventional structure

	Conventional structure	Structurally dissipating rock-shed of Essariaux
Impact energy	Maximal impact energy = 1800 kJ	ESLS impact = 1700 kJ (no significant irreversible damage) EULS impact = 3360 kJ (maximal impact energy)
Span	10 m	10 m
Ground thickness	4.70 m	0 m
Slab thickness	1 m	0.70 m
Deadweight	100,000 kg m^{-1}	17,500 kg m^{-1}
Bending reinforcements	96 cm^2 m^{-1}	40 cm^2 m^{-1}
Maintenance	Impossibility of removing the blocks of the embankment and of expanding the ground	Possibility of reaching above the slab to remove blocks and of repairing it

With the aim of developing a structure which is simple to build and has low construction costs, we introduce a new concept of rock-shed structures (Fig. 2) called structurally dissipating rock-shed (SDR). The main innovation of the SDR concept is to make the slab work in its plastic range under high energy impacts, but with a low frequency of occurrence (Mougin et al., 2005). The impact energy is dissipated directly by the actuation of the slab and by the plastic deformation of the concrete and reinforcements for impacts in the centre, and by the buckling of the fuse supports for impacts on the edges. After the high energy impacts, the slab may have to be repaired:

- for central shocks, by replacing the very fissured zone (demolition and reconstruction);
- for edge shocks, by changing the fuse supports which have buckled.

With low intensity shocks, which are more frequent, the slab undergoes no plastic damage and repairs are not necessary. The advantages are a significant reduction (approximately 30%) in the thickness of the slab and of a considerable reduction in the total deadweights, which leads to savings on the foundations system. Table 1 lists the advantages of an SDR compared to a conventional rock-shed.

This paper presents the experiments realized on an SDR model, carried out as part of the construction of the first work (SDR of Essariaux—Savoy—France), and the theoretical approach to design such a structure. With the intention of developing simplified methods of calculation, we will focus on the determination of percussion loads applied to the slab and on the punching effects.

2. General operating principle

In order to understand and to analyse the phenomena which occur during the impact of an element onto a flexible slab (Miyamoto et al., 1994; Shirai et al., 1997), it must be called to mind that many parameters have considerable influence on the loads (but is this notion of loads appropriate in a dynamics context?), on the damage mechanisms or on the modes of energy transfer. The parameters usually listed in literature are:

- materials of the two colliding elements,
- initial cracking or fractures,
- shape of the impactor,
- velocities,
- incidence angle of the impactor,
- rigidity of the structure hit.

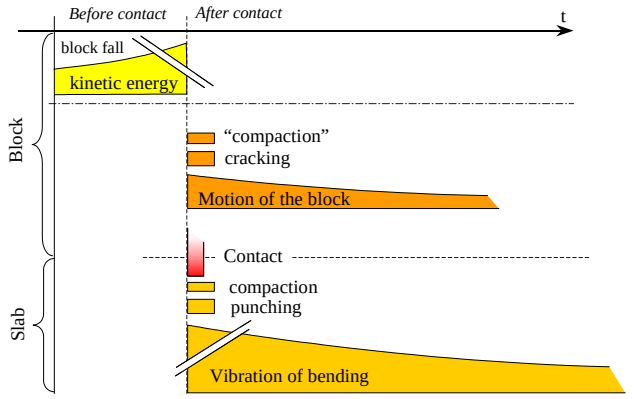

Fig. 3. Dissipation and damage mechanisms.

These parameters have highly variable influences according to the phenomena observed. When an impactor gets into contact with a (more or less rigid) structure, such as a slab, it is possible to observe various phenomena occurring more or less simultaneously. Understanding these phenomena will permit to work out the dimensioning of the structure.

The first difficulty consists in doing away with the traditional three-notion approach that civil engineers have "load-stress-design", so as to adopt a reasoning process in which the dynamic phenomena are taken into account.

Thanks to the experiments we carried out, we could observe three different models of operation: one based on the bending of the slab (Hughes and Al-Dafiry, 1995), one based on punching (Dinic and Perry, 1990) and the last one based on the damage done to concrete at the contact surface ("compaction") (Burlion et al., 2001). These phenomena do not occur simultaneously: punching and compaction seem to appear during contact time whereas the bending of the slab (combined with punching) begins just after the first contact. These three phenomena will have to be taken into account in the design of the structure. Therefore, we think that the bending will lead to the dimensioning of the longitudinal reinforcements, the punching to that of the shear reinforcements and to a lesser extent to that of the longitudinal reinforcements and finally the "compaction" to the characteristics of concrete.

Concerning the energy levels (transfer or dissipation), the three phenomena are not in the same order of magnitude. By computation, we could determine that "compaction" represents about 1–5% of the incidental energy and most of it is dissipated during the contact and by the bending of the slab. Fig. 3 represents the various kinds of energy dissipations occurring during a shock.

3. Experiments

3.1. Presentation of the model

The structure tested is a 1/3 scale model of the rock-shed, built in Savoie-France (Delhomme et al., 2003). It is made up of a horizontal slab of width 4.8 m, length 12 m, and thickness 0.28 m (Fig. 4). It is built with 30 MPa compressive strength concrete and is reinforced by a strong density of HA Fe E 500 steel reinforcements (4300 kg of steel for 16 m^3 of concrete). The slab is supported by 22 metal fuse supports (Fig. 5): they consist of a steel tube (TUE 220 A, 100 mm high, 70 mm in diameter and 2.9 mm thick)

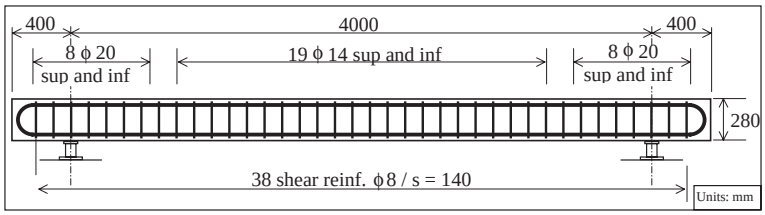

Fig. 4. Experimental slab.

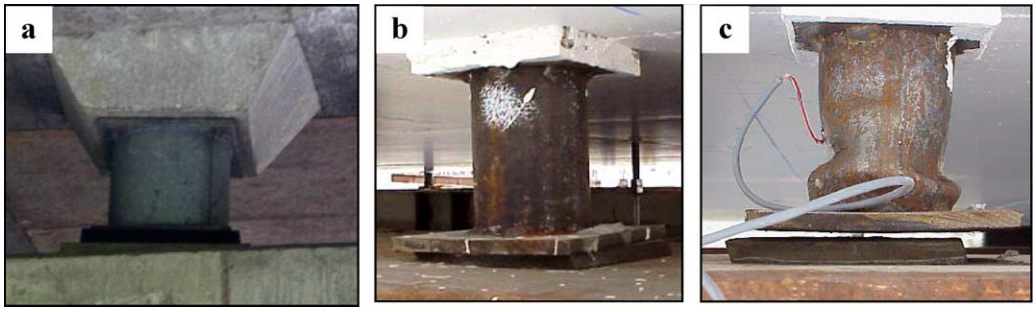

Fig. 5. Fuse supports: support of actual SDR (a), support of the structure tested (b), buckled support of the structure tested (c).

welded onto two $100 \times 100\ mm^2$, 8 mm thick plates; these fuses buckle under a static load of 260 kN. The slab simply laid on fuse supports which themselves are supported by neoprene plates.

3.2. Tests carried out

The SDR slab is intended to undergo several impacts during its lifetime and the types of impact fall into two classes:

- ESLS (''Equivalent Serviceability Limit States''): the loading should not create significant irreversible damage within the structure;
- EULS (''Equivalent Ultimate Limit States''): the loading creates significant irreversible damage which requires the structure to be repaired; this impact corresponds to the maximum energy level that the slab is able to withstand.

In order to simulate rock impact, the model is hit by a cubic reinforced concrete block (Fig. 6). The block was made of reinforced concrete, and not of steel, because the high density of steel involves a block of low dimensions which would not be equivalent to the size of a similar mass rock. The shape of the block is not spherical because a rock has several facets and consequently, a cubic block is closer to the reality. Moreover, a spherical block involved problems of reinforcement and concreting.

A block of about 450 kg is dropped from a 15 m height to simulate an ESLS loading (68 kJ) and from a 30 m height to replicate an EULS loading (135 kJ). A final destructive test is also carried out with a block of 810 kg released from a 37 m height (294 kJ).

A total number of six tests, with different impact locations (Fig. 7), were carried out during three experimental trial runs (Table 2).

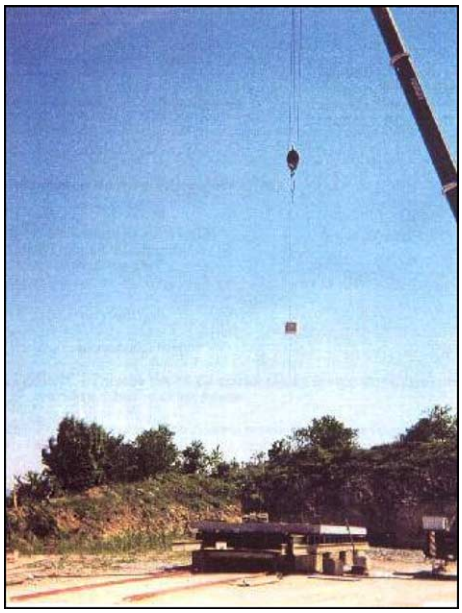

Fig. 6. Impact test.

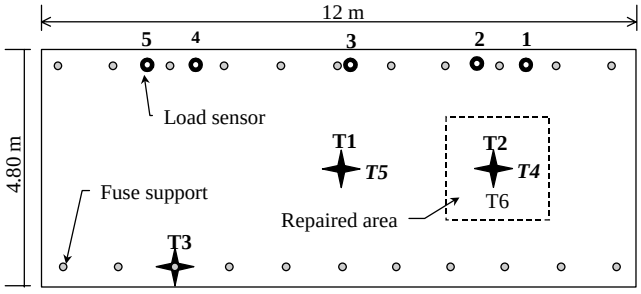

Fig. 7. Position of the impact tests.

Table 2
Characteristics of the different tests carried out on the experimental slab

Campaign	Test	State of the impacted area	Impact energy (kJ)	Impact position
C1	T1	Unused	68	Central area
	T2	Unused	135	Central area
	T3	Unused	135	On supports
C2	T4	Repaired after T2	138	Central area
	T5	Damaged by T3	134	Central area
C3	T6	Damaged by T4	294	Central area

To test a complete life cycle of the slab, it was repaired after test T2. The repair consists in demolishing and extracting the fissured concrete, which was done by hydro-demolition, using a very high pressure water

Fig. 8. Slab reinforcements after hydro-demolition.

jet: the concrete was carefully cut out and the network of steel reinforcements was exposed without damage (Fig. 8); then, the zone cleared was refilled with standard concrete (with 35 MPa compressive strength).

The examination of the reinforcements revealed that traction broke some shear reinforcements, showing that the punching load in the impact zone had been underestimated. Hence, the stirrups of 8 mm in diameter were all replaced by reinforcements of 10 mm in diameter (representing a 56% cross-section increase).

3.3. Instrumentation of the slab

The slab was equipped with a set of sensors connected to a data acquisition station whose sampling rate is 7000 Hz; the following sensors were installed:

- strain gauges on the lower and higher longitudinal reinforcements;
- strain gauges on the shear reinforcements to measure the traction strains at the time of impact;
- nine LVDT displacement sensors, with ± 50 mm measuring range, under the slab;
- seven accelerometers (frequency range between 0.5 and 10,000 Hz), ± 500 g near the impact and ± 50 g farther away, on the lower face of the slab, close to the LVDT sensors;
- one accelerometer (± 5000 g vertically) on the impacting block to measure impact deceleration. (frequency range between 1 and 10,000 Hz);
- five load sensors (capacity 1000 kN) regularly positioned under a line of fuse supports.

In complement to these sensors, a high-speed camera (1000 frames per second—2 m $\times$ 2 m field—256×240 pixels) was used to record the impact between the block and the slab.

4. Experiment and percussion analysis

4.1. Looking into theory

The product of a force by an elementary contact time "dt" is called elementary impulse "d$\vec{\tau}$". If the application time of the load ($\vec{F}$) becomes very small, the impulse ($\vec{\tau}$) becomes a shock or a percussion (Larralde, 1986):

$$\vec{\tau} = \int_{t_0}^{t_1} \vec{F}\,\mathrm{d}t \quad [t_0,\ t_1] \text{ being very small.} \tag{1}$$

For a body of mass "m" going up from velocity $\vec{v}_1$ to $\vec{v}_2$, without external force, this percussion is equal to the variation of the linear momentum which it generates:

$$\vec{\tau} = m(\vec{v}_2 - \vec{v}_1) \quad \vec{\tau} \text{ in N s} \tag{2}$$

When the impact is completely elastic (Timoshenko and Goodier, 1970), a symmetric load–time diagram is obtained and a full restitution is observed. The maximum impact load ($F_{\max}$) between a sphere (with mass "m" and impact velocity "v_{imp}") and a motionless plane can be described after Hertz's law (1896)s as follows:

$$F_{\max} = \left(\frac{5m}{4}\right)^{3/5} K^{2/5}\, v_{\text{imp}}^{6/5} \tag{3}$$

where K (=contact parameter) depends on the geometrical and elastic properties of the bodies.

A complete description of the response in a plastic contact zone is quite elaborate, but a relatively simple starting point is Meyer's law (Tabor, 1951). The variation of contact load "F" for the quasi-static indentation of a sphere of radius R, with the radius of permanent crater "a", is determined empirically by

$$F = ka^n \quad \text{with } k = \frac{C}{R^{n-2}} \tag{4}$$

where C and n are constants for a particular set of materials.

For a full plastic impact between a completely rigid sphere and a deformable plane ($n = 1$), the Eq. (4) is reduced to:

$$F = \pi p_0 (2R\delta - \delta^2) \tag{5}$$

or

$$F \approx 2\pi p_0 R\delta \tag{6}$$

where p_0 is the average contact pressure at the interface and δ the deformation of the contact zone.

A combination of Eq. (1) and the constant contact pressure hypothesis was employed to build an elasto-plastic model (Fig. 9): an initial elastic compression phase; an additional plastic deformation in a central region occurring at constant pressure p_0, surrounded by an elastic annulus; and a restitution process phase involving elastic recovery of the plastic zone (Jensen and Hoiseth, 1983; van Mier et al., 1991). There is no

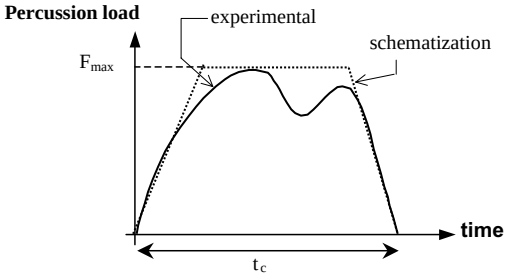

Fig. 9. Schematization of the variation of the percussion load.

elastic phase in the case of the penetration of a plane surface by a conical or pyramidal indenter, as plastic flow is generated instantaneously (Golsmith, 1960; Davis and Hunter, 1960). By neglecting the initial elastic mode and the restitution, the impact load can be regarded as constant:

$$F = \pi \sigma_0 a^2 \tag{7}$$

where $\sigma_0 = 3\,\sigma_y$ (σ_y = uniaxial compressive strength) and a = radius of the contact surface impactor-plane.

On the basis of Eq. (2) and supposing that the mass of the block is constant and that the slab is motionless:

$$F = \frac{m_i(v_{i,2} - v_{i,1})}{t_c} \tag{8}$$

where $v_{i,1}$ = impactor velocity before impact; $v_{i,2}$ = impactor velocity after impact; m_i = impactor mass; t_c = contact time; F = percussion load.

The calculation of the maximum percussion load boils down to the determination of impactor velocities and contact time.

4.2. Experimental analysis of percussion

Determining the impact load has been done for tests T4, T5 and T6. The recordings of the following sensors have been analysed as follows (Delhomme et al., 2003):

- A high-speed camera records the block hitting the slab. The frame analysis allows to determine the velocity of the center of gravity (c.o.g.) of the block.
- For tests T4 and T5, an LVDT displacement transducer is positioned under the slab vertically from the impact point. It records the vertical displacements of the slab. Thanks to this sensor, it is possible to know the slab velocity, by derivation of the displacements.
- For tests T4 and T6, an accelerometer is fastened to the impactor, to measure the vertical deceleration of the block during the shock. Due to the break in the connection, we were not able to measure the acceleration during the rebound.

The analysis of test T4 (Fig. 10) shows that the shock breaks down into the following stages (Fig. 11):

1. Period $[t_1, t_2]$: a block corner hits the slab and the block strongly decelerates. A first percussion load applies to the slab.
2. Period $[t_2, t_3]$: the block swings around its first impact point, its vertical deceleration is almost nil and the slab velocity decreases. The contact load between the block and the slab is near zero.
3. Period $[t_3, t_4]$: the whole side of the block hits the slab. The block decelerates and the slab velocity increases. A second percussion load applies.
4. After t_4: the block begins to separate from the slab which has reached its maximum vertical displacement.

An identical pattern can be observed in the other two tests (T5 and T6) because contact is never plane to plane.

We obtain the experimental percussion loads in Table 3 by using Eq. (8). The results of test T4 are given for the second contact time because the slant angle of the block is important and the second percussion load more significant than the first one. The percussion load of test T3 is supposed to be equal to the one of test T5 because the impact angles of the block and the impact energies are identical.

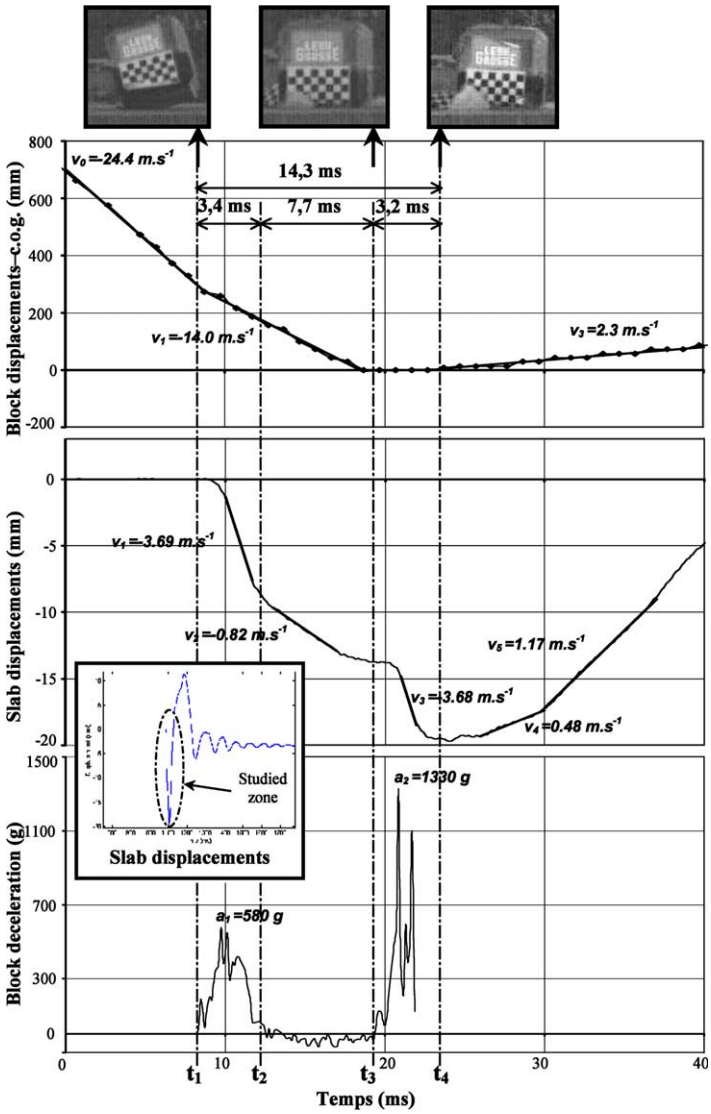

Fig. 10. Vertical displacement of the center of gravity of the block, slab vertical displacement under impact point, vertical block deceleration during test T4.

The percussion load is more important when impact is almost flat (test T5) rather than on an angle (test T4). The contact time of test T6 is very close to that of the first two tests (T3 and T4) and the increase in the percussion load is primarily due to the increase in the mass of the block.

4.3. Analysis of load sensors signals

Load sensor number 3, located under the support line, did not act in dynamics, therefore, it is not possible to express the total resultant of support reactions. However the analysis of sensors 2, perpendicular

Table 3
Maximal percussion loads for tests T3, T4, T5 and T6

Tests	Impact energy (kJ)	α[a] (°)	Velocity before impact (m s^{-1})	Velocity after impact (m s^{-1})	Contact time (ms)	Maximal percussion load (MN)
T4	138	20	14.0 ± 0.8	0 ± 0.02	3.2 ± 0.2	2.1 ± 0.2
T5–T3	134	5	23.5 ± 0.8	0 ± 0.02	3.6 ± 0.2	3.0 ± 0.2
T6	294	9	26.3 ± 0.8	0 ± 0.02	4.0 ± 0.2	5.3 ± 0.2

[a] To see Fig. 11.

to the impact point, and sensors 5, located at the end of the slab, (Fig. 12) makes it possible to draw the following conclusions:

- At the time of the shock, the supports located near the impact zone, unload. The start of their loading occurs 5 ms latter than the contact between the block and the slab. Moreover, we note that the loading peak is shifted by 120 ms between sensors 2 and 5. These phenomena prove that the structure cannot be

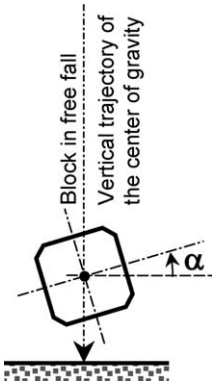

Fig. 11. Slanting of the block.

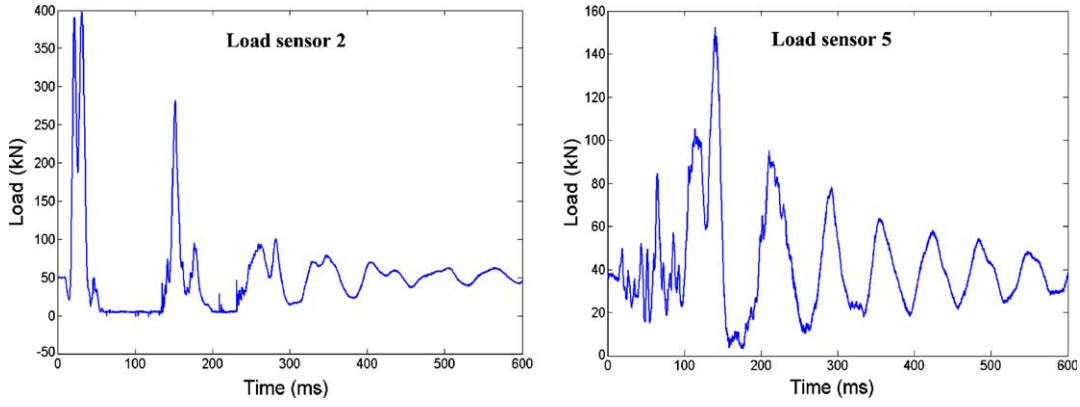

Fig. 12. Signals of load sensors number 2 and 5—Test T4.

regarded as rigid because the shock generates oscillations of the slab according to several modes, which are superimposed. A Fourrier analysis, without taking into account the first three pseudo-periods of the signal, revealed a first natural frequency of 16 Hz.
- Load sensor 2 indicates a null effort when the slab is bent to the top meaning that the slab raises from supports located near the impact point. Anti-rising mechanisms will have to be installed in order to avoid all risks of displacement.

5. Punching of the slab

5.1. Bibliography

In the bibliography (Theodorakopoulos and Swamy, 2002; CEB-FIP, 2001), the description of the kinematic process of the punching mechanism for a static loading is the following:

- formation of a roughly circular crack around loading area on the tension surface of the slab and its subsequent propagation into the compression zone in concrete;
- formation of new flexural cracks;
- initiation of an inclined crack.

With increasing loads the inclined crack develops towards the concrete and reaches the tension and compression reinforcements. In the final stage, the punching strength is expressed like the summation of each resisting vertical force in concrete and in steel (shear and flexural).

In this paper, only two methods are used:

- an analytical model by Menétrey (2002): it is the main model which takes the influence of the shear reinforcement into account;
- Eurocode 2 (2003) because it is the official European Code.

Menétrey's model is based on the summation of each resisting vertical force and the ultimate punching (F_{pun}) load is given by

$$F_{pun} = F_{ct} + F_{dow} + F_{sw} \tag{9}$$

where F_{ct} is the vertical component of the concrete tensile force, F_{dow} is the dowel-effect contribution to flexural reinforcement and F_{sw} is the shear reinforcement contribution.

Like Menétrey's model, the ultimate punching load with Eurocode 2 is obtained as a summation of a part of the punching shear capacity without shear reinforcement (concrete tensile force and dowel effect) and the contribution to the shear reinforcements.

$$V_{Rd,cs} = 0.75\ V_{Rd,c} + V_s \tag{10}$$

With

$$V_{Rdc} = v_{Rdc} u d \tag{11}$$

where u is the length of the critical perimeter, d is the mean effective depth, V_s is the contribution to the shear reinforcements, v_{Rdc} is the punching shear stress and coefficient 0.75 allows to take into account that the yielding of the shear reinforcements is not reached.

In order to compare Eurocode 2 and Menétrey's model, we have not included any partial safety factor. The angle of punching crack is 45° (our experimental observation) for Menétrey's model and 26.6° for EC2

Table 4
Ultimate punching loads computed with Eurocode 2 and Menétrey's model for different shear reinforcement diameters

	Menétrey		Eurocode 2	
Cracking angle (°)	45		26.6	
Effort	$V_c + V_{dow}$	V_{pun}	$V_c + V_{dow}$	V_{pun}
Current area $\varnothing_{shear\ reinf.} = 8$ mm	1.08 MN	2.69 MN	0.20 MN	2.22 MN
Repaired area $\varnothing_{shear\ reinf.} = 10$ mm	1.04 MN	3.56 MN	0.21 MN	3.42 MN

(imposed by this method). The dynamic effects were taken into account by increasing the yield strength of steel and concrete. Table 4 presents the punching loads computed with Menétrey's model and Eurocode 2 (Perrotin et al., 2004).

The influence of the shear reinforcements is dominant because they represent between 70% and 90% of the ultimate punching load. The results found with Menétrey's model and with Eurocode 2 are very close in spite of the fact that the cracking angles used are respectively 45° and 26.6°. Eurocode 2 takes into account a great number of shear reinforcements compared to Menétrey's model. On the other hand, an effective design strength is used in Eurocode 2 in order to consider the anchoring efficiency of stirrups.

5.2. Comparison of impact and punching loads

The statement of cracks (Fig. 13) reveals much more important damage under the slab for test T2 than for test T4. Moreover, after the hydro-demolition of the area impacted during test T2, we noted that five stirrups of eight millimetres in diameter were broken whereas the gages glued onto the shear reinforcements for test T4 (Fig. 14) recorded a maximum strain of 1940 $\mu m\ m^{-1}$ (lower than the yield strain of steel). The slab was markedly punched for test T2 while no damage due to punching was visible for test T4.

For test T6, a great part of the concrete cover under the slab was ejected. The demolition of the impacted zone revealed a 45° slanting crack in the concrete. Several shear reinforcements across this crack were broken by traction and the lower and upper reinforcements were strongly sheared (Fig. 15). Therefore, the slab was strongly punched by the block.

Table 5 compares the experimental observations with the impact load and punching load determined previously. We have considered that the ultimate punching load was reached when the shear reinforcements broke.

Each time we have observed shear reinforcement breaking (T3 and T6), the percussion loads were systematically higher than the ultimate punching load. For test T4, the maximal percussion load is lower than

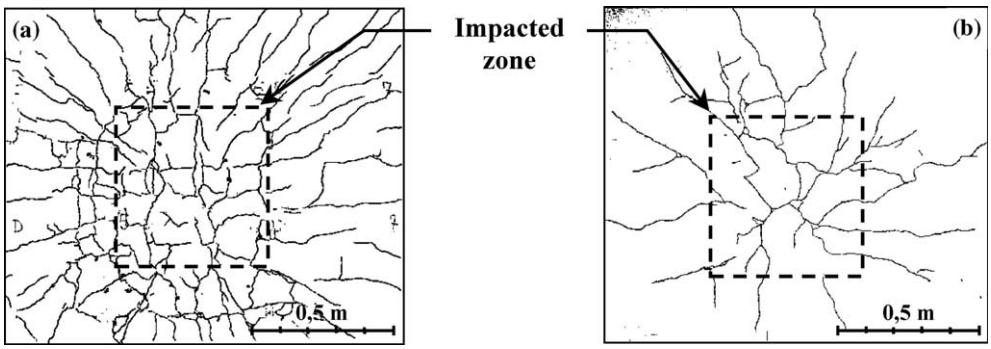

Fig. 13. Statements of cracking under the slab for tests T2 (a) and T4 (b).

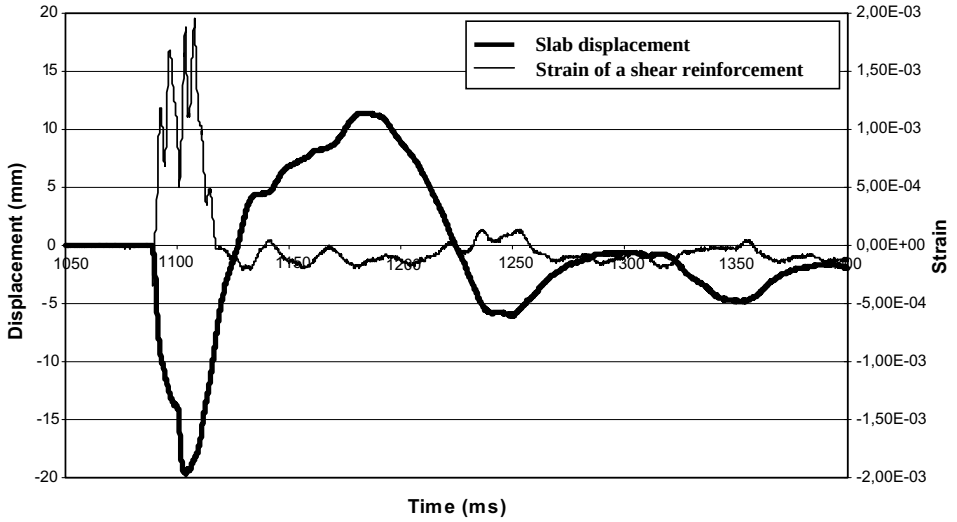

Fig. 14. Slab vertical displacement under the impact point and strains of a shear reinforcement crossing the inclined crack—Test T4.

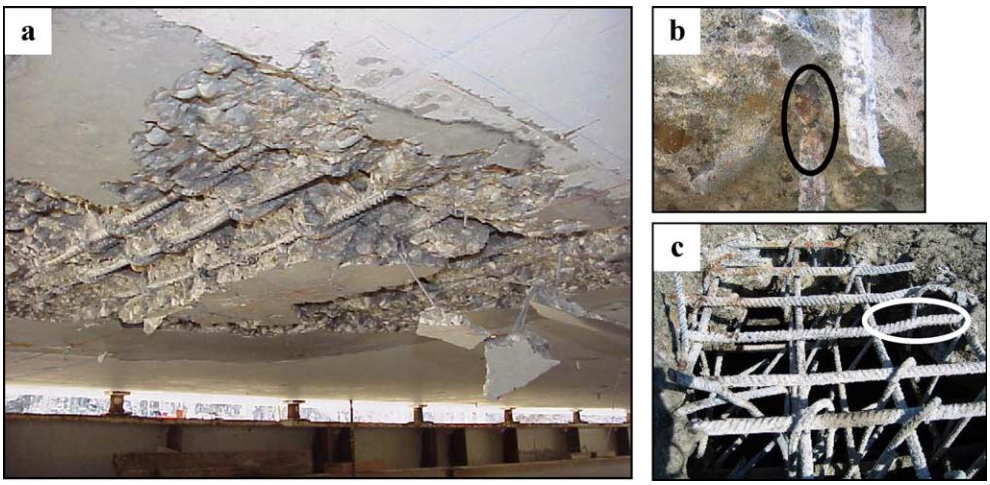

Fig. 15. State of the impacted zone after test T6: ejection of the concrete cover (a), breaking of a shear reinforcement (b), shearing of a superior reinforcement (c).

Table 5
Comparison between the ultimate punching loads, the maximal percussion loads and the visual observations for tests T3, T4, T5 and T6

Test	Shear reinforcement diameters (mm)	Energy (kJ)	Maximal percussion load (MN)	Punching load (MN) Menétrey's model	Break of shear reinforcements
T4	10	138	2.1	3.6	No
T5–T3	8	134	3	2.7	Yes
T6	10	294	5.2	3.6	Yes

the value of the punching load and we did not observe any punching phenomenon. Therefore, these models are a good estimate of what happens in reality.

6. Conclusions

Following the trial runs we conducted, we are able to validate the functioning principle of the Structurally Dissipating Rock-shed. Under low intensity shocks, the slab perfectly absorbs the impact energy while remaining in its elastic range. Under high energy level shocks, the system is significantly damaged: strong cracking around the impacts in the central zone of the slab, buckling of the supports for impacts on the edges. The repair method is simple to implement and efficient: the slab behavior remains identical after being repaired.

As the aim of this research is to develop simplified calculation methods that can be used in engineering offices, we can say that the slab is damaged according to two modes: by punching during the contact phase and by bending likely to create plastic strains.

A detailed analysis of punching and percussion phenomena shows that the percussion load of a block hitting an RC slab, assuming a perfectly plastic shock, could be determined experimentally from the variation of the linear momentum of the block and the contact time. This percussion load must be compared with the ultimate punching load, computed with Menétrey's model or Eurocode 2, in order to design the slab under punching.

To develop simplified design methods, concrete compaction in the contact area has yet to be analysed and the bending behaviour of the slab to be modelled, taking dynamic effects into account.

Acknowledgments

The writers wish to thank "TONELLO I.C." office, designer of the Structurally Dissipating Rock-sheds, and "Léon GROSSE" company for its support in the building of the slab. Sincere thanks are also extended to "CETE-LYON" laboratory for its cooperation in strain gauges preparation and to "SETRA" for its financial assistance.

References

Burlion, N., Pijaudier-Cabot, G., Dahan, N., 2001. Experimental analysis of compaction of concrete and mortar. International Journal for Numerical and Analytical Methods in Geomechanics 25, 1467–1486.

CEB-FIP, 2001. Punching of structural concrete slabs. Technical Report, Bulletin 12.

Davis, C.D., Hunter, S.C., 1960. Assessment of the strain-rate sensitivity of metals by indentation with conical intenders. Journal of Mechanics and Physics of Solids 8, 235.

Delhomme, F., Agbossou, A., Mommessin, M., Mougin, J.-P., Perrotin, P., 2003. Behavior study of a rock-shed slab. In: Proceedings of the 1st International Conference on Response of Structure under Extreme Loading, Toronto, Canada.

Delhomme, F., Perrotin, P., Mommessin, M., Mougin, J.-P., 2003. Impact on a RC rock-shed slab: percussion analysis. In: Proceedings of the 5th International Conference on Shock & Impact Loads on Structures, Changsha, China, 151–158.

Dinic, G., Perry, S.H., 1990. Shear plug formation in concrete slabs subjected to hard impact. Engineering Fracture Mechanics 35, 343–350.

Eurocode 2, 2003. Design of concrete structures-Part 1.1: General rules and rules for buildings. European Standard, April 2003.

Golsmith, W., 1960. Impact. Arnold Publication, London.

Hertz, H., 1896. On the contact of elastic solids. Miscellaneous Papers. Macmillan, London, Chapter 5, 146–183.

Hughes, B.P., Al-Dafiry, H., 1995. Impact energy absorption at contact zone and supports of reinforced plain and fibrous concrete beams. Construction and Building Materials 9, 239–244.

Ikeda, K., Kishi, N., Kawase, R., Konno, H., Nakano, O., 1999. A practical design procedure of three-layered absorbing system. In: Proceedings of the Joint Japan–Swiss Scientific Seminar, Department of Civil Engineering, Kanazawa University, Japan, pp. 113–119.

Jensen, J.J., Hoiseth, K., 1983. Impact of dropped objects on lightweight concrete. Nordic Concrete Research 2, 102–113.

Larralde, J.P., 1986. Dynamique. Masson Edition, pp. 301–328.

Masuya, H., Labiouse, V., 1999. Impact load by rock falls and design of protection structures. Proceedings of the Joint Japan–Swiss Scientific Seminar, Department of Civil Engineering, Kanazawa University, Japan.

Menétrey, P., 2002. Synthesis of punching failure in reinforced concrete. Cement and Concrete Composites 24, 497–507.

Miyamoto, A., King, M.W., Fujii, M., 1994. Integrated analytical procedure for concrete slabs under impact loads. Journal of Structure Engineering 120, 1685–1702.

Mougin, J.-P., Perrotin, P., Mommessin, M., Tonello, J., Agbossou, A., 2005. Rock fall impact on reinforced concrete slab: an experimental approach. International Journal of Impact Engineering 31, 169–183.

Perrotin, P., Delhomme, F., Mommessin, M., Mougin, J.-P., 2004. Behaviour of an impacted reinforced concrete slab: percussion and punching analysis. In: Proceedings of the 8th International Conference on Structures Under Shock and Impact, Crete, Greece, 419–427.

Shirai, T., Kambayashi, A., Ohno, T., Taniguchi, H., Ueda, M., Ishikawa, N., 1997. Experiment and numerical simulation of double-layered RC plates under impact loadings. Nuclear Engineering and Design 176, 195–205.

Tabor, D., 1951. The Hardness of Metals. Clarendon Press, Oxford.

Theodorakopoulos, D.D., Swamy, R.N., 2002. Ultimate punching shear strength analysis of slab-column connections. Cement and Concrete Composites 24, 509–521.

Timoshenko, S.P., Goodier, J.N., 1970. Theory of Elasticity, 3ème ed. McGraw-Hill, Singapore.

van Mier, J.G.M., Pruijssers, A.F., Reinhardt, H.W., Monnier, T., 1991. Load–time response of colliding concrete bodies. Journal of Structure Engineering 117, 354–374.